

Yet an other method to compute the thermodynamic Casimir force in lattice models

Martin Hasenbusch

Institut für Physik, Humboldt-Universität zu Berlin

Newtonstr. 15, 12489 Berlin, Germany

e-mail: Martin.Hasenbusch@physik.hu-berlin.de

Abstract

We discuss a method that allows to compute the thermodynamic Casimir force at a given temperature in lattice models by performing a single Monte Carlo simulation. It is analogous to the one used by de Forcrand and Noth and de Forcrand, Lucini and Vettorazzo in the study of 't Hooft loops and the interface tension in $SU(N)$ lattice gauge models in four dimensions. We test the method at the example of thin films in the XY universality class. In particular we simulate the improved two-component ϕ^4 model on the simple cubic lattice. This allows us to compare with our previous study, where we have computed the Casimir force by numerically integrating energy densities over the inverse temperature.

Keywords: λ -transition, Classical Monte Carlo simulation, thin films, finite size scaling, thermodynamic Casimir effect

1 Introduction

In 1978 Fisher and de Gennes [1] realized that when thermal fluctuations are restricted by a container a force acts on the walls of the container. Since this effect is similar to the Casimir effect, where the restriction of quantum fluctuations induces a force, it is called “thermodynamic” Casimir effect. Since thermal fluctuations only extend to large scales in the neighbourhood of a continuous phase transitions it is also called “critical” Casimir effect. Recently this effect has attracted much attention, since it could be verified for various experimental systems and quantitative predictions could be obtained from Monte Carlo simulations of spin models [2]. The neighbourhood of the critical point implies that the Casimir force is described by a universal finite size scaling function ¹. For the film geometry, finite size scaling predicts

$$F_{casimir}(L_0, t) \simeq \frac{k_B T}{L_0^3} \theta(t[L_0/\xi_0]^{1/\nu}) \quad (1)$$

where k_B is the Boltzmann constant, T the temperature, $t = (T - T_c)/T_c$ the reduced temperature and L_0 the thickness of the film. The amplitude ξ_0 of the correlation length in the high temperature phase is defined by

$$\xi \simeq \xi_0 t^{-\nu} \quad (2)$$

where ξ is the correlation length of the bulk system and ν its critical exponent. The function $\theta(x)$ is the same for all films in a given universality class, where also the boundary universality class [9] has to be taken into account.

As a first application of the numerical method discussed here, we study the improved two-component ϕ^4 model on the simple cubic lattice. The phase transition of this model belongs to the XY universality class in three dimensions. Also the λ -transition of ^4He shares this universality class. The experimental study of the λ -transition provided highly accurate estimates for critical exponents and amplitude ratios of the bulk system. For a review see [10]. Also confined systems have been studied in detail at the λ -transition of ^4He [11]. In particular, the thermodynamic Casimir force in thin films of ^4He has been measured [12, 13]. These experiments confirm that the thermodynamic Casimir force for films of different thickness L_0 can indeed be described by the same scaling function $\theta(x)$. For all temperatures the force turns out to be negative. In the high temperature phase $\theta(x)$ is monotonically decreasing with decreasing x . The Casimir force vanishes for large values of x .

¹For reviews on finite size scaling see [3, 4]; For reviews on critical phenomena and the Renormalization group see e.g. [5, 6, 7, 8].

At the critical point of the bulk system $\theta(0) = -0.07 \pm 0.03$ [12]. In the low temperature phase the finite size scaling function shows a minimum at $x_{min} \approx -5.5$ with $\theta_{min} \approx 1.3$ [13]. For $x < x_{min}$ the finite size scaling function increases with decreasing temperature. For small values of x it seems to approach a finite negative value.

It has been a challenge for theorists to compute the finite size scaling function $\theta(x)$. Krech and Dietrich [14, 15] have computed it in the high temperature phase using the ϵ -expansion up to $O(\epsilon)$. This result is indeed consistent with the measurements on ^4He films. Deep in the low temperature phase, the spin wave approximation should provide an exact result. It predicts a negative non-vanishing value for $\theta(x)$. However the experiments suggest a much larger absolute value for $\theta(x)$ in this region. Until recently a reliable theoretical prediction for the minimum of $\theta(x)$ and its neighbourhood was missing. Using a renormalized mean-field approach the authors of [16, 17] have computed $\theta(x)$ for the whole temperature range. Qualitatively they reproduce the features of the experimental result. However the position of the minimum is by almost a factor of 2 different from the experimental one. The value at the minimum is wrongly estimated by a factor of about 5.

Only quite recently Monte Carlo simulations of the XY model on the simple cubic lattice [18, 19, 20] provided results for $\theta(x)$ which essentially reproduce the experiments on ^4He films [12, 13]. In [21] we have applied the method used by [19] to study the improved two-component ϕ^4 model on the simple cubic lattice. The study of this model should provide more accurate results since corrections $\propto L_0^{-\omega}$ with $\omega = 0.785(20)$ [22] are eliminated. Essentially our result confirms those of [18, 19, 20]. However there is a discrepancy in the position x_{min} of the minimum of $\theta(x)$ that is clearly larger than the errors that are quoted: In [19] $x_{min} = -5.3(1)$ and in [20] $x_{min} = -5.43(2)$ which has to be compared with our result $x_{min} = -4.95(3)$ [21].

In order to verify our result [21] we compute the thermodynamic Casimir force in the two-component ϕ^4 model using a different method that is analog to that of [23, 24] used to compute the string tension and 't Hooft loops in lattice gauge model. The general idea is similar to that of [18, 20]. However, in contrast to [18, 20] a single simulation is sufficient ² to obtain the Casimir force at a given temperature.

This paper is organized as follows: First we define the ϕ^4 model on the simple cubic lattice. Then we discuss in detail the method used here to compute the thermodynamic Casimir force. In section 4 we discuss our numerical simulations. First we performed numerical simulations at the critical point of the three-dimensional

²Provided that f_{bulk} is known.

system. Next we computed the free energy density for the thermodynamic limit of the three-dimensional system at two values of the inverse temperature β in the high and the low temperature phase each. Then we have measured the thermodynamic Casimir force for $L_0 = 8.5$ at various temperatures. Finally we have simulated at x_{min} for the thicknesses $L_0 = 6.5, 7.5, 9.5, 12.5$ and 24.5 to complement our results of ref. [21]. Finally we summarize our results and give our conclusion.

2 The model and the observables

We study the two-component ϕ^4 model on the simple cubic lattice. We label the sites of the lattice by $x = (x_0, x_1, x_2)$. The components of x might assume the values $x_i \in \{1, 2, \dots, L_i\}$. We simulate lattices of the size $L_1 = L_2 = L$ and $L_0 \ll L$. In 1 and 2-direction periodic boundary conditions are used. In order to mimic the vanishing order parameter that is observed at the boundaries of ^4He films, free boundary conditions in 0-direction are employed. This means that the sites with $x_0 = 1$ and $x_0 = L_0$ have only five nearest neighbours. This type of boundary conditions could be interpreted as Dirichlet boundary conditions with 0 as value of the field at $x_0 = 0$ and $x_0 = L_0 + 1$. Note that viewed this way, the thickness of the film is $L_0 + 1$ rather than L_0 . This provides a natural explanation of the result $L_s = 1.02(7)$ obtained in [25]. The Hamiltonian of the two-component ϕ^4 model, for a vanishing external field, is given by

$$\mathcal{H} = -\beta \sum_{\langle x, y \rangle} \vec{\phi}_x \cdot \vec{\phi}_y + \sum_x \left[\vec{\phi}_x^2 + \lambda(\vec{\phi}_x^2 - 1)^2 \right] \quad (3)$$

where the field variable $\vec{\phi}_x$ is a vector with two real components. $\langle x, y \rangle$ denotes a pair of nearest neighbour sites on the lattice. The partition function is given by

$$Z = \prod_x \left[\int d\phi_x^{(1)} \int d\phi_x^{(2)} \right] \exp(-\mathcal{H}). \quad (4)$$

Note that following the conventions of our previous work, e.g. [26], we have absorbed the inverse temperature β into the Hamiltonian.³ In the limit $\lambda \rightarrow \infty$ the field variables are fixed to unit length; Hence the XY model is recovered. For $\lambda = 0$ we get the exactly solvable Gaussian model. For $0 < \lambda \leq \infty$ the model undergoes a second order phase transition that belongs to the XY universality class. Numerically, using

³Therefore, following [7] we actually should call it reduced Hamiltonian.

Monte Carlo simulations and high-temperature series expansions, it has been shown that there is a value $\lambda^* > 0$, where leading corrections to scaling vanish. Numerical estimates of λ^* given in the literature are $\lambda^* = 2.10(6)$ [27], $\lambda^* = 2.07(5)$ [26] and most recently $\lambda^* = 2.15(5)$ [22]. The inverse of the critical temperature β_c has been determined accurately for several values of λ using finite size scaling (FSS) [22].

We shall perform our simulations at $\lambda = 2.1$, since for this value of λ comprehensive Monte Carlo studies of the three-dimensional system in the low and the high temperature phase have been performed [25, 22, 28, 29]. At $\lambda = 2.1$ one gets $\beta_c = 0.5091503(6)$ [22]. Since $\lambda = 2.1$ is not exactly equal to λ^* , there are still corrections $\propto L_0^{-\omega}$, although with a small amplitude. In fact, following [22], it should be by at least a factor 20 smaller than for the standard XY model.

2.1 The energy density and the reduced free energy

Note that in eq. (3) β does not multiply the second term. Therefore, strictly speaking, β is not the inverse of $k_B T$. In order to study universal quantities it is not crucial how the transition line in the β - λ plane is crossed, as long as this path is not tangent to the transition line. Therefore, following computational convenience, we vary β at fixed λ . In the following equations it is understood that λ is kept fixed.

The reduced free energy density is defined as

$$f(\beta) \equiv -\frac{1}{L_0 L_1 L_2} [\log Z(\beta) - \log Z(0)] . \quad (5)$$

Note that compared with the free energy density \tilde{f} , a factor $k_B T$ is skipped. For convenience we have defined the reduced free energy such that $f(0) = 0$. For $\beta = 0$ the partition function factorizes and thus $\log Z(0)/(L_0 L_1 L_2)$ does not depend on the system size.

We define the (internal) energy density as the derivative of the reduced free energy density with respect to β . Furthermore, to be consistent with our previous work e.g. [30], we multiply by -1 :

$$E = \frac{1}{L_0 L_1 L_2} \frac{\partial \log Z}{\partial \beta} . \quad (6)$$

It follows

$$E = \frac{1}{L_0 L_1 L_2} \left\langle \sum_{\langle x, y \rangle} \vec{\phi}_x \cdot \vec{\phi}_y \right\rangle , \quad (7)$$

which can be easily determined in Monte Carlo simulations. From eqs. (5,6) it follows that the free energy density can be computed as

$$f(\beta) = f(\beta_0) - \int_{\beta_0}^{\beta} d\tilde{\beta} E(\tilde{\beta}) . \quad (8)$$

3 The numerical method

From a thermodynamic point of view, the Casimir force per unit area is given by

$$F_{casimir} = -k_B T \frac{\partial f_{ex}}{\partial L_0} \quad (9)$$

where L_0 is the thickness of the film and $f_{ex} = f_{film} - L_0 f_{bulk}$ is the reduced excess free energy per area of the film. In lattice models the thickness L_0 assumes only integer values. Therefore we have to approximate the derivative by a finite difference $F_{casimir}(L_0, t) \approx -k_B T \Delta f_{ex}(L_0, t)$, where

$$\Delta f_{ex}(L_0, t) \equiv f(L_0 + 1/2, t) - f(L_0 - 1/2, t) - f_{bulk}(t) \quad (10)$$

where $L_0 + 1/2$ is integer. $f(L_0 + 1/2, t)$ and $f(L_0 - 1/2, t)$ are the reduced free energies of films of the thicknesses $L_0 + 1/2$ and $L_0 - 1/2$, respectively, and $f_{bulk}(t)$ is the reduced free energy density of the three-dimensional bulk system. The main numerical task is to compute the difference of the reduced free energy per area for films of the thickness $L_0 - 1/2$ and $L_0 + 1/2$.

In order to compute this difference, it is useful to have the same number of field-variables for both systems. To this end, we add $L_1 \times L_2$ isolated sites to the film of the thickness $L_0 - 1/2$. Isolated means that the field $\vec{\phi}$ at such a site is subject to the potential $\vec{\phi}^2 + \lambda(\vec{\phi}^2 - 1)^2$ but the interaction with other sites is missing. Using our definition (5), adding isolated sites to the film does not change the free energy per area. Let us denote the partition function of this system by $\bar{Z}_{L_0-1/2}$. Now we can express the difference of the reduced free energies as

$$\begin{aligned} F(L_0 + 1/2, t) - F(L_0 - 1/2, t) &= \log \frac{\bar{Z}_{L_0-1/2}}{Z_{L_0+1/2}} \\ &= \log \frac{D[\phi] \exp(-H_{L_0+1/2}) \exp(-\beta \sum_{\langle x,y \rangle \in [L_0+1/2]} \vec{\phi}_x \vec{\phi}_y)}{D[\phi] \exp(-H_{L_0+1/2})} \\ &= \log \left\langle \exp(-\beta \sum_{\langle x,y \rangle \in [L_0+1/2]} \vec{\phi}_x \vec{\phi}_y) \right\rangle_{L_0+1/2} , \end{aligned} \quad (11)$$

where $\langle x, y \rangle \in [L_0 + 1/2]$ denotes the sum over all nearest neighbour pairs, where at least one of the sites is an element of the layer $x_0 = L_0 + 1/2$. Formally we have rewritten the difference of free energies as an expectation value. The problem is that the observable is strongly fluctuating and therefore it is impossible to obtain an accurate estimate from a Monte Carlo simulation of the film of the thickness $L_0 + 1/2$. A well known method to overcome this problem is the so called “multistage sampling” strategy; see e.g. [31]. This means that a sequence of systems is introduced that interpolates between the two we are interested in. These systems are characterized by the Hamiltonians H_0, H_1, \dots, H_N , where we identify $H_0 = \bar{H}_{L_0-1/2}$ and $H_N = H_{L_0+1/2}$. Now we can rewrite the ratio of partition functions as

$$\frac{Z_0}{Z_N} = \frac{Z_0}{Z_1} \frac{Z_1}{Z_2} \dots \frac{Z_{N-1}}{Z_N} . \quad (12)$$

where we can write the factors as

$$z_{i+1} \equiv \frac{Z_i}{Z_{i+1}} = \langle \exp(-H_{i+1} + H_i) \rangle_{i+1} \quad (13)$$

and hence

$$F(L_0 + 1/2, t) - F(L_0 - 1/2, t) = \sum_{i=1}^N \log z_i . \quad (14)$$

If the sequence is properly chosen and N sufficiently large, the fluctuations of $\exp(-H_{i+1} + H_i)$ are small and the expectation value can be accurately determined from the simulation of the system $i + 1$.⁴ Obviously there is much freedom in the construction of the sequence of systems. A straight forward one is given by

$$H_i = \bar{H}_{L_0-1/2} + \frac{i}{N} \beta \sum_{\langle x, y \rangle \in [L_0+1/2]} \vec{\phi}_x \vec{\phi}_y . \quad (15)$$

This choice is very similar to the one used by [18, 20]. The main difference is that these authors did consider as starting system a film of thickness $L_0 - 1/2$ plus a two-dimensional system of the size $L_1 \times L_2$. This means that in contrast to our choice the intra-layer couplings are switched on.

Here we use a different interpolation. It is inspired by a method used to compute the string tension and 't Hooft loops in lattice gauge theories [23, 24].

⁴It might be even better to express the difference as an expectation value in a system that is between i and $i + 1$.

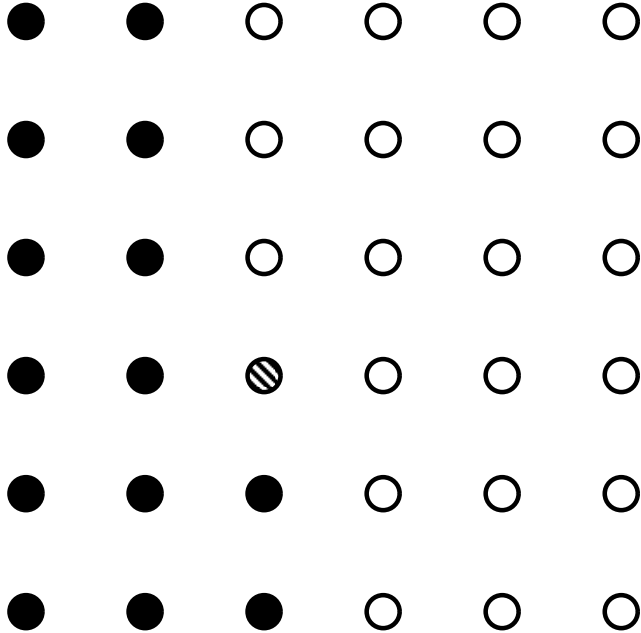


Figure 1: We sketch the layer $x_0 = L_0 + 1/2$ of our system. In the sketch $L_1 = L_2 = 6$. The sites are given by circles. The filled ones are coupled to the system, while the empty ones are isolated. We compute the free energy difference between the system, where the shaded circle is isolated and the system, where it is coupled to the film. For a discussion see the text.

We add the isolated sites one by one to the film. In the step $i = x_1 L_2 + x_2$ the site $x = (L_0 + 1/2, x_1, x_2)$ is added. All sites that are added are coupled with their nearest neighbours that are already in the film. This way we have constructed a sequence of $L_1 \times L_2 + 1$ systems. Hence, $L_1 \times L_2$ independent Monte Carlo simulations have to be performed to obtain $F(L_0 + 1/2, t) - F(L_0 - 1/2, t)$. Following [23, 24] this can however be avoided: With increasing L_1, L_2 the sum (14) is dominated by contributions where the newly added site is far from the boundaries in 1 and 2-direction. Hence most of the contributions are essentially equal to that for $x_1 = L_1/2$ and $x_2 = L_2/2$ as sketched in figure 1. In the limit $L_1, L_2 \rightarrow \infty$, this should become exact. Hence only a single simulation for $x_1 = L_1/2$ and $x_2 = L_2/2$ is required.

Usually updates are performed on the whole lattice ⁵ before a measurement

⁵In the Monte Carlo slang this is often called “sweep”.

of the observables is performed. However in the present case, the observable is localized at a single site. Therefore the effort for the measurement and the update would be highly unbalanced. To circumvent this problem, one would like to update the fields in the neighbourhood of this site more frequently than those far off. In order to achieve this we follow the idea presented in [32]: We consider a sequence of sub-sets of the sites of the lattice. Here, the smallest set consists of the site $(L_0 + 1/2, L_1/2, L_2/2)$ only. The next larger one consists of $(L_0 + 1/2, L_1/2, L_2/2)$ and its three neighbours $(L_0 + 1/2, L_1/2 - 1, L_2/2)$, $(L_0 + 1/2, L_1/2, L_2/2 - 1)$ and $(L_0 - 1/2, L_1/2, L_2/2)$. The larger ones are given by blocks of the size $b_l \times (2b_l + 1) \times (2b_l + 1)$ and $L_0 \times (2b_l + 1) \times (2b_l + 1)$ if $b_l > L_0$. These blocks are centred around the site $(L_0 + 1/2, L_1/2, L_2/2)$. If $b_l < L_0$, the eight corners of these blocks are $(L_0 + 1/2, L_1/2 - b_l, L_2/2 - b_l)$, $(L_0 + 1/2, L_1/2 - b_l, L_2/2 + b_l)$, $(L_0 - 1/2, L_1/2 - b_l, L_2/2 + b_l)$, $(L_0 - 1/2, L_1/2 + b_l, L_2/2 + b_l)$, $(L_0 + 1/2 - b_l, L_1/2 - b_l, L_2/2 - b_l)$, $(L_0 + 1/2 - b_l, L_1/2 - b_l, L_2/2 + b_l)$, $(L_0 + 1/2 - b_l, L_1/2 + b_l, L_2/2 + b_l)$ and $(L_0 + 1/2 - b_l, L_1/2 + b_l, L_2/2 + b_l)$. In our simulations we have used $b_l = 1, 2, 3, 5, 10, 20, 40, 80, \dots$, where the largest b_l is chosen such that $b_l < L_1, L_2$.

In a certain sequence, Metropolis and overrelaxation sweeps⁶ over these sub-sets are performed. This sequence, which we shall call one update cycle, is best explained by the following pseudo-code

```
cluster_update(); metrosweep(full lattice); oversweep(full lattice);
for(i1=0; i1 < m_1; i1++)
{
  metrosweep(b_1); oversweep(b_1);
  for(i2=0; i2 < m_2; i2++)
  {
    metrosweep(b_2); oversweep(b_2);
    .
    .
    .
    for(iM=0; iM < m_M; iM++)
    {
      metrosweep(b_M); oversweep(b_M);
      measure();
    }
    .
    .
  }
```

⁶We have implemented these updates as discussed in appendix A of [26]

·
}
}

We did not perform an accurate tuning of the parameters $m_1, m_2, m_3, \dots, m_M$; instead we have chosen them such that the CPU-time spent at each block-size is roughly the same.

In the case of the single cluster-updates [33] it is easy to focus on the site $(L_0 + 1/2, L_1/2, L_2/2)$. One simply starts the clusters at the site $(L_0 + 1/2, L_1/2, L_2/2)$ instead of choosing the starting point at random. In our numerical tests we have not yet implemented this idea.

3.1 The measurement

The measurement consists in its most naive implementation in the evaluation of

$$A = \exp(-\beta \vec{\phi}_{(L_0+1/2, L_1/2, L_2/2)} \cdot \vec{\Phi}_{(L_0+1/2, L_1/2, L_2/2)}) \quad (16)$$

where

$$\vec{\Phi}_{(L_0+1/2, L_1/2, L_2/2)} = \vec{\phi}_{(L_0+1/2, L_1/2-1, L_2/2)} + \vec{\phi}_{(L_0+1/2, L_1/2, L_2/2-1)} + \vec{\phi}_{(L_0-1/2, L_1/2, L_2/2)} \quad (17)$$

We have reduced the variance by performing the integral over the angle of the field $\vec{\phi}_{(L_0+1/2, L_1/2, L_2/2)}$ exactly. This results in the improved observable

$$\bar{A} = \frac{1}{\int_0^{2\pi} d\alpha \exp(-R \cos \alpha)} = \frac{1}{2\pi I_0(R)} \quad (18)$$

where

$$R = \beta |\vec{\phi}_{(L_0+1/2, L_1/2, L_2/2)}| |\vec{\Phi}_{(L_0+1/2, L_1/2, L_2/2)}| \quad (19)$$

and $I_0(R)$ is a modified Bessel function. For our simulations we have tabulated $1/(2\pi I_0(R))$ for $0 \leq R \leq 3$ with a step-size of 0.0001, i.e. for 30001 values of R . During the simulation we then evaluated $1/(2\pi I_0(R))$ for $0 \leq R \leq 3$ by quadratically interpolating the results given in the table. If $R > 3$ we have evaluated the integral in eq. (18) numerically. A sufficient precision can already be achieved with about 30 nodes.

The expectation value

$$z = \langle A \rangle = \langle \bar{A} \rangle \quad (20)$$

is estimated by averaging \bar{A} over all measurements that we performed after thermalization. Here we have dropped the subscript $i = (L_1/2)L_2 + L_2/2$ of eq. 13, since only this value of i will be considered in the following. During the simulation we have averaged already all measurements in a given update cycle. These averages were written to a file. The statistical error was then computed taking into account the integrated autocorrelation time of these cycle averages.

4 Numerical Results

First we have simulated at the critical temperature of the bulk system. Next we have determined the reduced free energy of the bulk system at $\beta = 0.49$ and $\beta = 0.5$ in the high temperature phase and at $\beta = 0.533$ and $\beta = 0.56$ in the low temperature phase. For $L_0, L_1, L_2 \gg \xi$ the reduced free energy of the bulk system is given by $f_{bulk} = \log z$. Our new results are consistent with those obtained by integrating the energy densities computed in [30]. Then we have studied films of the thickness $L_0 = 8.5$ at four temperatures in the low temperature phase of the bulk system. Also here we find that the results are consistent with those of [30]. Finally we have simulated the thicknesses $L_0 = 6.5, 7.5, 9.5, 12.5$ and 24.5 at x_{min} . These simulations complement our results of [30] at x_{min} .

As random number generator we have used the SIMD-oriented Fast Mersenne Twister algorithm [34].

4.1 Simulations at the critical point

First we performed simulations at the inverse critical temperature $\beta_c = 0.5091503(6)$ of the three-dimensional system using lattices of the thicknesses $L_0 = 8.5, 12.5, 16.5, 24.5, 32.5$ and 64.5 . In all cases we have chosen $L_1 = L_2 = 12.5 \times (L_0 - 1/2)$. Since the correlation length of the film is $\xi_{2nd, film}/L_{0, eff} \approx 0.416$ [30] this should be sufficient to keep deviations from the two-dimensional thermodynamic limit smaller than our statistical errors. As a check we have simulated for $L_0 = 8.5$ in addition $L_1 = L_2 = 20, 30$ and 50 . We find $z = 0.84950517(36), 0.84951362(36)$ and $0.84951572(37)$ for these lattice sizes, respectively. Indeed, starting from $L_1 = L_2 = 30$ our results are consistent within error bars. Our results for $L_1 = L_2 = 12.5 \times (L_0 - 1/2)$ are summarized in table 1. In these simulations we have used block sizes up to $b_1 = 10, 20, 20, 40, 40$ and 80 for $L_0 = 8.5, 12.5, 16.5, 24.5, 32.5$ and 64.5 , respectively. For all these thicknesses and for all block-sizes we have used $m_l = 6$. The number of update cycles is 21349600, 7738500, 7700000, 2040000,

Table 1: Results for z at $\beta_c = 0.5091503$ [22] for lattices of the size $L_1 = L_2 = 12.5 \times L_0$.

L_0	z
8.5	0.84951552(24)
12.5	0.84947657(16)
16.5	0.84946525(23)
24.5	0.84945897(13)
32.5	0.84945717(16)
64.5	0.84945602(14)

1308200 and 281700 for $L_0 = 8.5, 12.5, 16.5, 24.5, 32.5$ and 64.5 , respectively. In total these simulations took about 16 month of CPU-time on a single core of a Quad-Core Opteron(tm) 2378 CPU (2.4 GHz).

The reduced excess free energy behaves as

$$f_{ex}(L_0, t) = L_{0,eff}^{-2} h(t[L_0/\xi_0]^{1/\nu}) + b(t) \quad (21)$$

where $L_{0,eff} = L_0 + L_s$ with $L_s = 1.02(7)$ [25] takes into account corrections due to the Dirichlet boundary conditions and $b(t)$ gives the effect of the Dirichlet boundary conditions on the analytic part of the free energy of the film. For a discussion and references see [35]. Taking the derivative with respect to L_0 at $t = 0$ we arrive at

$$-\left. \frac{\partial f_{ex}(L_0, t)}{\partial L_0} \right|_{t=0} = 2h(0)L_{0,eff}^{-3} = \theta(0)L_{0,eff}^{-3} \quad (22)$$

where θ is the finite size scaling function of the thermodynamic Casimir force.

It follows

$$\log z(L_0, \beta_c) = f_{ns}(\beta_c) - \theta(0)L_{0,eff}^{-3}. \quad (23)$$

Note that in the thermodynamic limit the singular part of the free energy density vanishes at the critical point; hence $f_{bulk}(\beta_c) = f_{ns}(\beta_c)$. The results of our fits are given in table 2.

In order to estimate the effect of the error of L_s on our results we have repeated these fits using $L_s = 0.95$. E.g. for $L_{0,min} = 12.5$ we get $f_{ns} = -0.16315930(10)$ and $\theta(0) = -0.0593(5)$. We have also checked the effect of the error of β_c . To this end we have computed $\Delta f(L_0, 0.5091509)$ by using the data for the energy given in

Table 2: Results for fits with the ansatz (23), where we have used $L_s = 1.02$ as input. All data for $L_0 \geq L_{0,min}$ are fitted. For a discussion see the text.

$L_{0,min}$	f_{ns}	$\theta(0)$	$\chi^2/\text{d.o.f.}$
8.5	-0.16315935(9)	-0.0606(3)	0.20
12.5	-0.16315932(10)	-0.0603(6)	0.14
16.5	-0.16315930(12)	-0.0597(17)	0.15

table 1 of [35]. We find that the effect on f_{ns} and $\theta(0)$ is small and can be ignored here. Based on the result obtained for $L_{0,min} = 12.5$ we take as final results

$$f_{ns} = -0.1631593(1) \quad , \quad \theta(0) = -0.060(2) \quad (24)$$

where the error-bar covers both the statistical error as well as the error due to the uncertainty of L_s .

This can be compared with the result for ^4He films $\theta(0) = -0.07 \pm 0.03$ [12], the ϵ -expansion up to $O(\epsilon)$: $\theta(0) = -0.044$ taken from table I of [14] and the estimate $\theta(0) = -0.062(5)$ obtained from Monte Carlo simulations of the standard XY model [19]. The authors of [36] quote $h(0) \simeq -0.03$ (in their notation Δ^f) as final result. All these results are consistent with ours. The largest discrepancy is seen for the ϵ -expansion. However one should note that in [19, 21] it has been observed that in the high temperature phase for $x \gtrsim 1$ the numerical result for θ matches nicely with the ϵ -expansion [14].

4.2 Free energy density of the bulk system

Here we compute the free energy density of the bulk system for two values of β in the high temperature phase and two values of β in the low temperature phase. These results are compared with ones obtained by integrating the energy density starting from $\beta_c = 0.5091503$ using the start value $f(\beta_c) = -0.1631593(1)$ obtained above.

For sufficiently large L_0 , L_1 and L_2 the quantity $\log z$ should be a good approximation of the bulk free energy density. In particular in the high temperature phase, this should be the case for $L_0, L_1, L_2 \gg \xi_{3D}$. Here we performed simulations at $\beta = 0.49$ where $\xi_{2nd,3D} = 3.72370(19)$ and $\beta = 0.5$ where $\xi_{2nd,3D} = 6.1498(5)$ (see table 5 of [29]).

At $\beta = 0.49$ we have simulated $L_0 = 49.5$, $L_1 = L_2 = 50$ and $L_0 = 99.5$, $L_1 = L_2 = 100$. For $L_0 = 49.5$, $L_1 = L_2 = 50$ we have used block sizes up to $b_1 = 20$ and $m_l = 6$. From 5203000 cycles we get $f(0.49) = -0.14712079(18)$. For $L_0 = 99.5$, $L_1 = L_2 = 100$ we have used block sizes up to $b_1 = 40$ and $m_l = 6$. From 945000 cycles we get $f(0.49) = -0.14712095(17)$. As expected, these results are indeed consistent within error bars and hence a good approximation of the thermodynamic limit.

Based on the experience gained at $\beta = 0.49$ we have simulated at $\beta = 0.5$ only the lattice size $L_0 = 99.5$, $L_1 = L_2 = 100$. We have used block sizes up to $b_1 = 20$ and $m_l = 6$. From 598000 cycles we get $f(0.5) = -0.15519942(24)$.

In the low temperature phase we find from simulations of a 199.5×500^2 lattice $f(0.533) = -0.18931867(66)$ and $f(0.56) = -0.22693625(73)$. We have used blocks up to the size $b_1 = 80$ and $m_l = 6$ for all block sizes. We performed 24700 and 21700 cycles for $\beta = 0.533$ and $\beta = 0.56$, respectively. Both of these simulations took about 8 weeks of CPU-time on a single core of a Quad-Core Opteron(tm) 2378 CPU (2.4 GHz).

Now we can check whether these results for the free energy density are consistent with those obtained from integrating the energy density [30] using eq. (3).

In [30] we have computed the energy density of the three-dimensional bulk system in the range of inverse temperatures $0.49 \leq \beta \leq 0.58$. We have fitted these data in the range $0.49 \leq \beta \leq 0.529$ with the ansatz

$$E(\beta) = E_{ns} + C_{ns}(\beta - \beta_c) + a_{\pm}|\beta - \beta_c|^{1-\alpha} + d_{ns}(\beta - \beta_c)^2 + b_{\pm}|\beta - \beta_c|^{2-\alpha} \quad (25)$$

where E_{ns} , C_{ns} , $\beta_c = 0.5091503(6)$ and $\alpha = -0.0151(3)$ [22] are input and a_{\pm} , d_{ns} and b_{\pm} are the 5 free parameters of the fit. For $\beta < 0.529$ we have integrated this ansatz, using the results for the fit-parameter obtained in [30]. In all cases we have taken $\beta_0 = \beta_c = 0.5091503$ as starting point of the integration, where we have used the estimate of $f(\beta_c)$ obtained above. Our results are summarized in table 3. For $\beta > 0.529$ we performed a numerical integration of the energy density using the trapezoidal rule, starting from $\beta_0 = 0.52$. The estimate for $f(0.52)$ is taken from table 3. We have checked that our result virtually does not depend on the choice of β_0 , where we switch from the integration of the ansatz (25) to the numerical integration of the energy density. Also the results for $\beta > 0.529$ are given in table 3. The error quoted is dominated by the error for the free energy at β_c .

In table 3 we also give our results for the free energy density of the bulk system at $\beta = 0.49, 0.50, 0.533$ and 0.56 as computed by the new method discussed here. We find that the results are consistent within error-bars. This confirms that we

Table 3: Numerical results for the free energy density of the bulk system. These were obtained by integration of the energy density. As starting point of the integration we have taken the critical point β_c and the value $f(\beta_c)$ obtained in the previous subsection. In addition in the third column we give estimates of the free energy density obtained directly with the method discussed in the present work.

β	f INTEGRAL	f DIRECT
0.49	-0.1471210(1)	-0.1471210(2)
0.50	-0.1551994(1)	-0.1551994(2)
0.51463	-0.1684460(1)	
0.52	-0.1740847(1)	
0.52348	-0.1779533(1)	
0.5301	-0.1857405(1)	
0.533	-0.1893183(1)	-0.1893187(7)
0.53814	-0.1958961(2)	
0.54	-0.1983478(2)	
0.54432	-0.2041851(2)	
0.56	-0.2269362(2)	-0.2269363(7)

can indeed compute the free energy density of the bulk system with 6 to 7 accurate digits.

4.3 Films of the thickness $L_0 = 8.5$

We have simulated at $\beta = 0.52, 0.533, 0.54, 0.56$ in the low temperature phase of the three-dimensional system. We have taken lattices of the size $L_1 = L_2 = 50, 100, 250, 500$ and 1000 to control corrections to the two-dimensional thermodynamic limit of the thin film. The simulations for $L = 1000$ took about 18 days of CPU time each. In table 4 we give our results for $-\Delta f_{ex}$, where we have used the estimates of f_{bulk} computed in section 4.2. At $\beta = 0.52$ the results for all choices of $L_1 = L_2$ are consistent within error-bars. At $\beta = 0.533$ a clear deviation of the results from those obtained for larger lattices can be observed up to $L_1 = L_2 = 100$. The result for $L = 500$ deviates by a bit more than two standard deviations from that for $L = 1000$, while the results for $L = 250$ and $L = 1000$ are consistent within error bars. For $\beta = 0.54$ and $\beta = 0.56$ the results obtained for $L = 250, 500$ and 1000 are consistent within error-bars. We conclude that in all cases for $L = 1000$ the

Table 4: Numerical results for minus the derivative of the excess free energy $-\Delta f_{ex}$ of films of the thickness $L_0 = 8.5$. In the last row we give the results of [21] for comparison.

$L \setminus \beta$	0.52	0.533	0.54	0.56
50	-0.0007423(14)	-0.0014878(23)	-0.0010417(27)	-0.0003621(23)
100	-0.0007432(8)	-0.0015797(13)	-0.0011867(18)	-0.0003870(13)
250	-0.0007436(5)	-0.0015845(8)	-0.0012564(14)	-0.0003934(8)
500	-0.0007439(3)	-0.0015863(5)	-0.0012679(10)	-0.0003940(5)
1000	-0.0007433(3)	-0.0015846(5)	-0.0012666(11)	-0.0003945(6)
ref. [21]	-0.0007392(18)	-0.0015795(24)	-0.0012600(26)	-0.0003874(28)

deviation from the thermodynamic limit is smaller than the error bar.

For comparison we give in the last row results [21] which were obtained by numerical integration of Monte Carlo data for ΔE_{ex} . We see that the results of [21] are about 0.000004 larger than our present ones. This deviation is about twice the statistical error. In [21] we have started the integration at $\beta = 0.49$ for $L_0 = 8.5$, setting $\Delta f_{ex}(0.49) = 0$. From the ϵ -expansion [14] we get $\theta(x) \approx -0.0039$ for $x = t[L_{0,eff}/\xi_0]^{1/\nu}$ corresponding to $\beta = 0.49$ and $L_0 = 8.5$. Hence $-\Delta f_{ex} = \theta L_{0,eff}^{-3} \approx -0.0000041$ which fully explains the difference observed in table 4.

4.4 The minimum of the Casimir force

In [21] we have determined the position of the minimum of θ for a large number of thicknesses of the film. To this end we have determined the zero of

$$\Delta E_{ex}(L_0, \beta) = E(L_0 + 1/2, \beta) - E(L_0 - 1/2, \beta) - E_{bulk}(\beta) \quad (26)$$

where $E(L_0 + 1/2, \beta)$ is the energy per area of a film of the thickness $L_0 + 1/2$ and $E_{bulk}(\beta)$ the energy density of the three-dimensional bulk system. We had simulated at a few values of β in the neighbourhood of β_{min} . To get a preliminary estimate of β_{min} we used the information gained already from the simulations for $L_0 = 8.5, 16.5$ and 32.5 , where we have simulated a large range of β -values and the ansatz $\beta_{min}(L_0) - \beta_c \simeq L_{0,eff}^{-1/\nu}$. These results are given in table 5, which we have copied from table 2 of [21]. In the present work, we have added the values of θ_{min} for $L_0 = 6.5, 7.5, 9.5, 12.5$ and 24.5 that were missing in [21]. To this end, we have simulated lattices of the size $L_1 = L_2 = 500$ for $L_0 = 6.5$ and 7.5 , $L_1 = L_2 = 1000$

Table 5: The position β_{min} of the minimum of the Casimir force and its value $-\Delta f_{ex,min}$ as a function of the thickness L_0 . In the present work we have completed the table by adding $\Delta f_{ex,min}$ for $L_0 = 6.5, 7.5, 9.5, 12.5$, and 24.5 .

L_0	β_{min}	$-\Delta f_{ex,min}$
6.5	0.54432(2)	-0.0032744(13)
7.5	0.53814(2)	-0.0022305(11)
8.5	0.53354(2)	-0.001582(3)
9.5	0.53010(2)	-0.0011714(8)
12.5	0.52348(2)	-0.0005468(6)
16.5	0.51886(2)	-0.0002494(11)
24.5	0.51463(2)	-0.0000803(3)
32.5	0.51279(2)	-0.0000348(5)

for $L_0 = 9.5$ and $L_0 = 12.5$, and $L_1 = L_2 = 2000$ for $L_0 = 24.5$. From these simulation we get $\log z$, while f_{bulk} is taken from table 3. Our results for $-\Delta f_{ex}$ are given in table 5.

Let us briefly discuss the simulation of the $L = 24.5$ film: The simulations took about 2 month of CPU-time on a single core of a Quad-Core Opteron(tm) 2378 CPU (2.4 GHz). We performed 33000 update cycles. We have used block sizes up to $b_1 = 160$ and $m_l = 6$ for all block sizes.

First we have fitted the results for $-\Delta f_{ex,min}$ given in the third column of table 5 with the ansatz

$$-\Delta f_{ex,min} = \theta_{min}(L_0 + L_s)^{-3} \quad (27)$$

where θ_{min} and L_s are the free parameters of the fit. Our results are summarized in table 27.

The $\chi^2/\text{d.o.f.}$ is smaller than 1 starting from $L_{0,min} = 8.5$, where all data with $L_0 \geq L_{0,min}$ are included into the fit. We find $L_s \approx 0.89$ which is a bit smaller than our previous result $L_s = 1.02(7)$ [25]. Note that already in [21] we observed that $L_s = 0.95$ apparently leads to a better matching of the data than $L_s = 1.02$.

To check the possible effect of sub-leading corrections we have fitted our data also with the ansatz

$$-\Delta f_{ex,min} = \theta_{min}(1 + cL_0^{-2})(L_0 + L_s)^{-3} . \quad (28)$$

Note that there a number of different corrections with an correction exponent close

Table 6: We have fitted the minimum of the thermodynamic Casimir force with the ansatz (27)

$L_{0,min}$	θ_{min}	L_s	$\chi^2/\text{d.o.f.}$
6.5	-1.299(2)	0.849(5)	2.64
7.5	-1.305(3)	0.864(7)	1.64
8.5	-1.313(5)	0.889(13)	0.89
9.5	-1.310(5)	0.880(15)	0.34
12.5	-1.312(9)	0.888(33)	0.50

Table 7: We have fitted the minimum of the Casimir force with the ansatz (28)

$L_{0,min}$	θ_{min}	L_s	c	$\chi^2/\text{d.o.f.}$
6.5	-1.322(8)	0.953(3)	1.08(35)	1.13
7.5	-1.320(10)	0.945(5)	0.97(61)	1.40

to 2. E.g. $\propto L_0^{-\omega'}$ with $\omega' = 1.8(2)$ [37] or the restoration of the symmetries that are broken by the lattice. Our results are summarized in table 28.

Now the value $L_s \approx 0.95$ is fully consistent with our previous result [25]. As final result we quote $\theta_{min} = -1.31(2)$, where we have estimated the systematic error by the difference of the two fits (27,28). This result fully confirms our previous estimate $\theta_{min} = -1.31(3)$ [21].

5 Summary and Conclusion

We have discussed a method to compute the thermodynamic Casimir force in lattice models which is closely related with the one used by de Forcrand and Noth [23] and de Forcrand, Lucini and Vettorazzo [24] in the study of 't Hooft loops and the interface tension in $SU(N)$ lattice gauge models in four dimensions.

We have tested the method at the example of thin films of the improved two-component ϕ^4 model on the simple cubic lattice. This model shares the XY universality class with the λ -transition of ^4He . Therefore the Casimir force that is measured for thin films of ^4He [12, 13] should be governed by the same universal finite size scaling function θ as that computed from lattice models in the XY

universality class.

Only quite recently θ has been obtained from Monte Carlo simulations of the standard XY model on the simple cubic lattice [18, 19, 20]. This result is of particular interest, since other theoretical methods do not provide us with accurate results for θ for the whole range of the scaling variable $x = t[L_0/\xi_0]^{1/\nu}$. Overall one finds a reasonable match between the experimental and Monte Carlo results. In [21] we have redone the Monte Carlo simulations using the improved two-component ϕ^4 model on the lattice. It turns out that there is a discrepancy in the position x_{min} of the minimum of $\theta(x)$: $x_{min} = -5.3(1)$ [19] and $x_{min} = -5.43(2)$ [20] have to be compared with our result $x_{min} = -4.95(3)$ [21].

The purpose of the present work is twofold: First we like to figure out the performance of the method and secondly we like to check and to complement the results of [21]. In particular:

We have accurately computed the finite size scaling function of the thermodynamic Casimir force $\theta(0)$ at the critical point of the three-dimensional bulk system. Our result is consistent with the experimental result for ^4He films [12] and previous Monte Carlo simulations [19, 36]. On the other hand there is a clear discrepancy with the ϵ -expansion [14].

We have demonstrated that the method even allows to compute the free energy density of the bulk system. However it seems to be more efficient in this case to integrate the energy density (3).

We have not worked out theoretically how fast $\log z$ converges to $\lim_{L_1, L_2 \rightarrow \infty} [f(L_0 + 1/2, t) - f(L_0 - 1/2, t)]$. A natural guess is that the convergence is exponentially fast in L_1, L_2 in the high temperature phase of the film, while in the low temperature phase it follows a power law. For the thickness $L_0 = 8.5$ we have simulated at four values of β for a large range of $L_1 = L_2$ up to $L_1 = L_2 = 1000$. The results show that the convergence with $L_1, L_2 \rightarrow \infty$ is no problem in practice. Our final results for $-\Delta f_{ex}$ at these four values of β are consistent but more accurate than those obtained in [21].

Finally we have computed θ_{min} for several thicknesses, where we have taken the values of x_{min} from [21]. This allowed us to improve the estimate $\theta_{min} = 1.31(3)$ [21] to $\theta_{min} = 1.31(2)$. This part of the study nicely shows that the virtues of the two method are complementary.

We have not worked out theoretically how the numerical effort increases for a given precision with increasing thickness of the film. We also have not optimised the parameters of the algorithm. However it is quite clear from the simulations presented here that the method, using our ad hoc choice of the parameters, is competitive with previous proposals.

Here we have tested the method at the example of the XY universality class. The application to other universality classes, like the Ising or Heisenberg universality class is straight forward. On the other hand, the method seems to be restricted to films with Dirichlet boundary conditions.

6 Acknowledgements

This work was supported by the DFG under the grant No HA 3150/2-1.

References

- [1] Fisher M E and de Gennes P-G, *Phenomena at the walls in a critical binary mixture*, 1978 CR Acad. Sci. Paris **B 287** 207
- [2] Gambassi A, *The Casimir effect: From quantum to critical fluctuations*, 2009 J. Phys. Conf. Series **161** 012037
- [3] M. N. Barber Finite-size Scaling in *Phase Transitions and Critical Phenomena*, Vol. 8, eds. C. Domb and J. L. Lebowitz, (Academic Press, 1983)
- [4] *Finite Size Scaling and Numerical Simulation of Statistical Systems*, ed. V. Privman, (World Scientific, 1990)
- [5] Wilson K G and Kogut J, *The renormalization group and the ϵ -expansion*, 1974 Phys. Rep. C **12** 75
- [6] Fisher M E, *The renormalization group in the theory of critical behavior*, 1974 Rev. Mod. Phys. **46** 597
- [7] Fisher M E, *Renormalization group theory: Its basis and formulation in statistical physics*, 1998 Rev. Mod. Phys. **70** 653
- [8] Pelissetto A and Vicari E, *Critical Phenomena and Renormalization-Group Theory*, 2002 Phys. Rept. **368** 549 [arXiv:cond-mat/0012164]
- [9] H. W. Diehl, Field-theoretical Approach to Critical Behaviour at Surfaces in *Phase Transitions and Critical Phenomena*, edited by C. Domb and J.L. Lebowitz, Vol. 10 (Academic, London 1986) p. 76.

- [10] Barmatz M, Hahn I, Lipa J A, and Duncan R V, *Critical phenomena in microgravity: Past, present, and future*, 2007 Rev. Mod. Phys. **79** 1
- [11] Gasparini F M, Kimball M O, Mooney K P, and Diaz-Avila M, *Finite-size scaling of ^4He at the superfluid transition*, 2008 Rev. Mod. Phys. **80** 1009
- [12] Garcia R and Chan M H W, *Critical Fluctuation-Induced Thinning of ^4He Films near the Superfluid Transition*, 1999 Phys. Rev. Lett. **83** 1187
- [13] Ganshin A, Scheidemantel S, Garcia R, and Chan M H W, *Critical Casimir Force in ^4He Films: Confirmation of Finite-Size Scaling*, 2006 Phys. Rev. Lett. **97** 075301
- [14] Krech M and Dietrich S, *Free energy and specific heat of critical films and surfaces*, 1992 Phys. Rev. A **46** 1886
- [15] Krech M and Dietrich S, *Specific heat of critical films, the Casimir force and wetting films near end points*, 1992 Phys. Rev. A **46** 1922
- [16] Zandi R, Shackell A, Rudnick J, Kardar M and Chayes L, *Thinning of superfluid films below the critical point*, 2007 Phys. Rev. E **76** (2007) 030601 [cond-mat/0703262]
- [17] Maciolek A, Gambassi A, and Dietrich S, *Critical Casimir effect in superfluid wetting films*, 2007 Phys. Rev. E **76** 031124 [cond-mat/0705.1064]
- [18] Vasilyev O, Gambassi A, Maciolek A, and Dietrich S, *Monte Carlo simulation results for critical Casimir forces*, 2007 Europhys. Lett. **80** 60009 [arXiv:0708.2902]
- [19] Hucht A, *Thermodynamic Casimir Effect in ^4He Films near T_c : Monte Carlo Results*, 2007 Phys. Rev. Lett. **99** 185301 [arXiv:0706.3458]
- [20] Vasilyev O, Gambassi A, Maciolek A, and Dietrich S, *Universal scaling functions of critical Casimir forces obtained by Monte Carlo simulations*, 2009 Phys. Rev. E **79** 041142 [arXiv:0812.0750]
- [21] Hasenbusch M, *The thermodynamic Casimir effect in the neighbourhood of the lambda-transition: A Monte Carlo study of an improved three dimensional lattice model* J. Stat. Mech. (2009) P07031 [arXiv:0905.2096]

- [22] Campostrini M, Hasenbusch M, Pelissetto A, and Vicari E, *Theoretical estimates of the critical exponents of the superfluid transition in He4 by lattice methods*, 2006 Phys. Rev. B **74** 144506 [cond-mat/0605083]
- [23] de Forcrand P and Noth D, *Precision lattice calculation of $SU(2)$ 't Hooft loops*, 2005, Phys. Rev. D **72** 114501 [hep-lat/0506005]
- [24] de Forcrand P, Lucini B and Vettorazzo M, *Measuring interface tensions in 4d $SU(N)$ lattice gauge theories* Nucl.Phys.Proc.Suppl.140:647-649,2005. [arXiv:hep-lat/0409148]
- [25] Hasenbusch M, *Kosterlitz-Thouless transition in thin films: A Monte Carlo study of three-dimensional lattice models*, 2009 J. Stat. Mech. P02005 [arXiv:0811.2178]
- [26] Campostrini M, Hasenbusch M, Pelissetto A, Rossi P, and Vicari E, *Critical behavior of the three-dimensional XY universality class*, 2001 Phys. Rev. B **63** 214503 [cond-mat/0010360]
- [27] Hasenbusch M and Török T, *High precision Monte Carlo study of the 3D XY-universality class*, 1999 J. Phys. A **32** 6361 [cond-mat/9904408]
- [28] Hasenbusch M, *The three-dimensional XY universality class: A high precision Monte Carlo estimate of the universal amplitude ratio A_+/A_-* , 2006 J. Stat. Mech. P08019 [cond-mat/0607189]
- [29] Hasenbusch M, *A Monte Carlo study of the three-dimensional XY universality class: Universal amplitude ratios*, J. Stat. Mech. (2008) P12006 [arXiv:0810.2716]
- [30] Hasenbusch M, *The specific heat of thin films near the λ -transition: A Monte Carlo study of an improved three-dimensional lattice model*, 2009 [arXiv:0904.1535]
- [31] Mon K K, 1985, *Direct Calculation of Absolute Free Energy for Lattice Systems by Monte Carlo Sampling of Finite-Size Dependence* Phys.Rev.Lett. **54** 2671
- [32] Caselle M, Hasenbusch M, and Panero M, *String effects in the 3d gauge Ising model*, 2003 JHEP **0301** 057 [arXiv:hep-lat/0211012]
- [33] Wolff U, *Collective Monte Carlo Updating for Spin Systems*, 1989 Phys. Rev. Lett. **62** 361

- [34] Saito M, *An Application of Finite Field: Design and Implementation of 128-bit Instruction-Based Fast Pseudorandom Number Generator*, PhD thesis, Dept. of Math., Graduate School of Science, Hiroshima University, Advisor: M. Matsumoto; The numerical program and a detailed description can be found at “<http://www.math.sci.hiroshima-u.ac.jp/~m-mat/MT/SFMT/index.html>”
- [35] Hasenbusch M, *The specific heat, the energy density and the thermodynamic Casimir force in the neighbourhood of the lambda-transition*, 2009 [arXiv:0907.2847]
- [36] Mon K K and Nightingale M P, *Critical surface free energies and universal finite-size scaling amplitudes of three-dimensional XY models by direct Monte Carlo sampling*, Phys. Rev B 35 (1987) 3560.
- [37] Newman K E and Riedel E K, *Critical exponents by the scaling-field method: The isotropic N-vector model in three dimensions*, 1984 Phys. Rev. B **30** 6615